MOS Device Modeling at 77 K

SIEGFRIED SELBERHERR, SENIOR MEMBER, IEEE

Abstract—**The state of the art in self-consistent numerical low-temperature MOS modeling is reviewed. The physical assumptions that are required to describe carrier transport at low ambient temperatures are discussed. Particular emphasis is put on the models for space charge (impurity freeze-out), carrier mobility (temperature dependence of scattering mechanisms at a semiconductor–insulator interface), and carrier generation-recombination (impact ionization). The differences with regard to the numerical methods required for the solution of low-temperature models compared to room-temperature models are explained. Typical results obtained with the simulator MINIMOS 4 are presented. These include comparisons of short-channel effects and hot-electron phenomena such as energy relaxation and avalanche breakdown at 77 and 300 K ambient temperature.**

I. Introduction

DEVICE modeling based on the self-consistent solution of fundamental semiconductor equations dates back to the famous work of Gummel in 1964 [33]. However, the first application of this rigorous style of modeling for problems at low ambient temperature (usually liquid-nitrogen temperature) was carried out first by Gaensslen *et al.* about 12 years later in 1976 [29]. The main reason for this delay cannot only be seen in the lesser demands for low-temperature simulation. Today not only supercomputers are made for operation at liquid-nitrogen temperature, such as the ETA-10 [25], but also microprocessors, cf. [19]. The primary reason for the fairly poor status in full numerical low-temperature device modeling stems from considerably increased difficulties regarding physical assumptions and implementation of the numerical solution.

II. Physical Aspects

A. Basic Equations

The model for hot-carrier transport used in any numerical device simulation is based on the well known fundamental semiconductor equations (1)–(5). There are ongoing arguments in the scientific community whether these equations are adequate to describe transport in submicrometer devices. Particularly the current relations (4) and (5), which are the most complex equations out of the set of the basic semiconductor device equations, undergo strong criticism in view of, for instance, ballistic transport [37], [51]. Their derivation from more fundamental physical principles is indeed not at all straightforward. They appear therefore with all sorts of slight variations in the specialized literature, and a vast number of papers has been published where some of their subtleties are dealt with. The interested reader is referred to, e.g., [9], [13], [28], [58]. Anyway, recent investigation on ultrashort MOSFET's [52] do not give evidence that it is necessary to waive these well established basic equations for silicon devices down to feature sizes in the order of 0.1 μm [60].

$$\operatorname{div}(\epsilon \cdot \operatorname{grad} \psi) = -\rho \tag{1}$$

$$\operatorname{div} \vec{J}_n - q \cdot \frac{\partial n}{\partial t} = q \cdot R \tag{2}$$

$$\operatorname{div} \vec{J}_p + q \cdot \frac{\partial p}{\partial t} = -q \cdot R \tag{3}$$

$$\vec{J}_n = q \cdot \mu_n \cdot n \cdot \left(\vec{E} + \frac{1}{n} \cdot \operatorname{grad} \left(n \cdot \frac{k \cdot T_n}{q} \right) \right) \tag{4}$$

$$\vec{J}_p = q \cdot \mu_p \cdot p \cdot \left(\vec{E} - \frac{1}{p} \cdot \operatorname{grad} \left(p \cdot \frac{k \cdot T_p}{q} \right) \right). \tag{5}$$

These equations include a set of parameters that have to be appropriately modeled in order to correctly describe the various transport phenomena qualitatively and quantitatively.

B. Modeling Space Charge

Poisson's equation (see (1)) requires a model for the space charge ρ that makes use of only the dependent variables ψ, n, p and material properties. The well established approach for this model is to sum up the concentrations with the adequate charge sign multiplied with the elementary charge as:

$$\rho = q \cdot (p - n + N_D^+ - N_A^-). \tag{6}$$

Here the first difference between room-temperature and low-temperature simulation becomes apparent. The doping concentration $N_D^+ - N_A^-$ is usually assumed to be fully ionized at room temperature, which intuitively does not hold for low-temperature analysis. The classical way to describe partial ionization is based on the formulas

$$N_D^+ = \frac{N_D}{1 + 2 \cdot \exp\left(\frac{E_{fn} - E_D}{k \cdot T} \right)}$$

$$N_A^- = \frac{N_A}{1 + 4 \cdot \exp\left(\frac{E_A - E_{fp}}{k \cdot T} \right)} \tag{7}$$

Manuscript received September 27, 1988; revised December 5, 1988. This work was supported by the Research Laboratories of Siemens AG, Munich, Germany; the Research Laboratories of the Digital Equipment Corporation, Hudson, NY; and by the Fond zur Förderung der wissenschaftlichen Forschung under Contract S43/10.

The author is with the Institut für Mikroelektronik, Technical University of Vienna, Gusshausstrasse 27-29, A-1040 Vienna, Austria.

IEEE Log Number 8926651.

where E_D and E_A are the ionization energies of the respective donor and acceptor dopant. Typical values for $E_c - E_D$ and $E_A - E_v$ for the most common dopants in silicon are: 0.054 eV for arsenic, 0.045 eV for phosphorus, 0.039 eV for antimony, and 0.045 eV for boron. A quite complete list can be found in [65]. These ionization energies are recommended to be modeled as doping dependent in [17]; however, it seems not to be important for MOSFET's regarding my experience. Note that only energy differences can be given (E_c and E_v are the conduction band and the valence band energy, respectively). Next the Fermi levels E_{fn} and E_{fp} have to be appropriately related to the dependent variables by making use of Fermi statistics.

$$n = N_c \cdot \frac{2}{\sqrt{\pi}} \cdot F_{1/2}\left(\frac{E_{fn} - E_c}{k \cdot T}\right)$$

$$p = N_v \cdot \frac{2}{\sqrt{\pi}} \cdot F_{1/2}\left(\frac{E_v - E_{fp}}{k \cdot T}\right) \tag{8}$$

where N_c and N_v are the density of states in the conduction band and the valence band, respectively. The classical formulas for the density of states are given by

$$N_c = 2 \cdot \left(\frac{2 \cdot \pi \cdot k \cdot T \cdot m_n^*}{h^2}\right)^{3/2}$$

$$N_v = 2 \cdot \left(\frac{2 \cdot \pi \cdot k \cdot T \cdot m_p^*}{h^2}\right)^{3/2}. \tag{9}$$

$F_{1/2}(x)$ is the Fermi function of order 1/2, which is defined by

$$F_{1/2}(x) = \int_0^\infty \frac{\sqrt{y}}{1 + e^{y-x}} \cdot dy. \tag{10}$$

The parameters m_n^* and m_p^*, which are the effective masses for electrons and holes, respectively, now have to be modeled to be able to evaluate the formulas for the density of states (see (9)). Probably the most elaborate models that are fits to experimental values date back to Gaensslen *et al.* [29], [31].

$$m_n^* = m_o \cdot \left(1.045 + 4.5 \cdot 10^{-4} \cdot \left(\frac{T}{\mathrm{K}}\right)\right) \tag{11}$$

$$m_p^* = m_o \cdot \left(0.523 + 1.4 \cdot 10^{-3} \cdot \left(\frac{T}{\mathrm{K}}\right) - 1.48 \cdot 10^{-6} \cdot \left(\frac{T}{\mathrm{K}}\right)^2\right). \tag{12}$$

These fitting expressions are claimed to be valid over the range from 50 to 350 K. A graphical representation is given in Fig. 1.

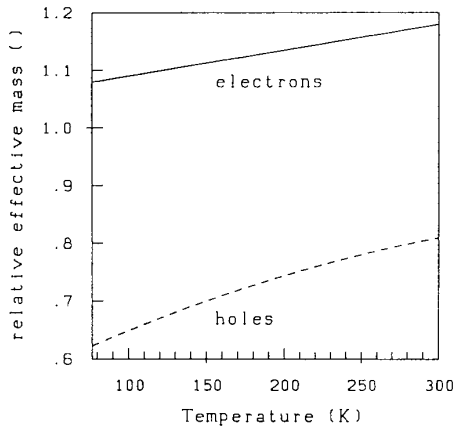

Fig. 1. Relative effective masses versus temperature in silicon.

It is worthwhile to note that the ratio of the density of states depends only on the ratio of the effective masses.

$$\frac{N_c}{N_v} = \left(\frac{m_n^*}{m_p^*}\right)^{3/2}. \tag{13}$$

By means of some simple algebraic manipulation with the expressions for the carrier concentrations (see (8)), we obtain:

$$\frac{E_{fn} - E_D}{k \cdot T} = G_{1/2}\left(\frac{n}{N_c}\right) + \frac{E_c - E_D}{k \cdot T} \tag{14}$$

$$\frac{E_A - E_{fp}}{k \cdot T} = G_{1/2}\left(\frac{p}{N_v}\right) + \frac{E_A - E_v}{k \cdot T}. \tag{15}$$

$G_{1/2}(x)$ is the inverse Fermi function of order 1/2 defined with

$$G_{1/2}\left(\frac{2}{\sqrt{\pi}} \cdot F_{1/2}(x)\right) = x. \tag{16}$$

It is now possible by evaluating the expressions for the density of states (given in (9)) with fits to the effective masses (given in (11) and (12)) to compute numerical values for the ionized impurity concentrations (see (7)) using only the carrier concentrations, which are the dependent variables in the basic equations. However, comparisons to experiment indicate that it is better to compute the density of states from (13) and a fit to the intrinsic carrier concentration of (17).

$$n_i = \sqrt{N_c \cdot N_v} \cdot \exp\left(-\frac{E_g}{2 \cdot k \cdot T}\right). \tag{17}$$

E_g is the bandgap $E_c - E_v$, which can be modeled temperature dependent with the fit provided by Gaensslen *et al.* [29], [31]. Note that most publications that present (18) contain a typographical error. The linear temperature coefficient for E_g below 170 K is $1.059 \cdot 10^{-5}$ eV and not

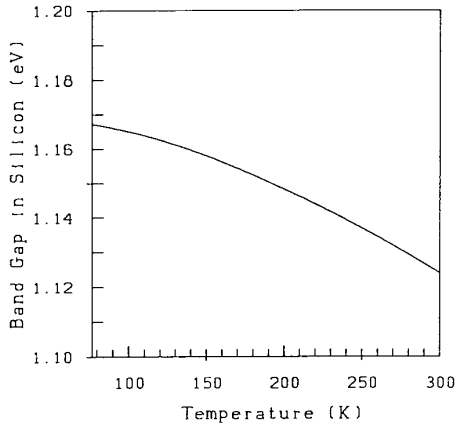

Fig. 2. Energy bandgap versus temperature in silicon.

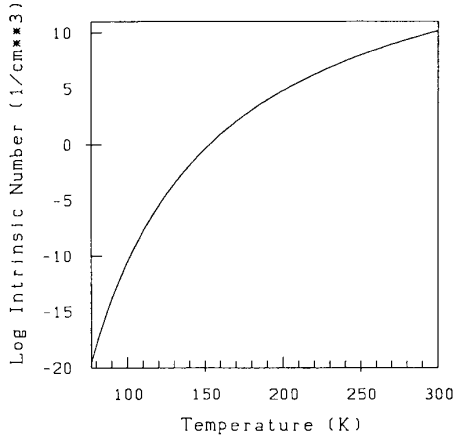

Fig. 3. Intrinsic carrier concentration versus temperature in silicon.

as usually found, $1.059 \cdot 10^{-6}$ eV [40]. A graphical representation of (18) is given in Fig. 2.

$$E_g = \begin{cases} 1.17\ \text{eV} + 1.059 \cdot 10^{-5}\ \text{eV} \cdot \left(\frac{T}{\text{K}}\right) \\ \quad - 6.05 \cdot 10^{-7}\ \text{eV} \cdot \left(\frac{T}{\text{K}}\right)^2, \quad T \le 170\ \text{K} \\ 1.1785\ \text{eV} - 9.025 \cdot 10^{-5}\ \text{eV} \cdot \left(\frac{T}{\text{K}}\right) \\ \quad - 3.05 \cdot 10^{-7}\ \text{eV} \cdot \left(\frac{T}{\text{K}}\right)^2, \quad T > 170\ \text{K}. \end{cases} \tag{18}$$

The prefactor in (17) can be fitted to experiments by (19). With these data one obtains an intrinsic carrier concentration as given with Fig. 3. Note the well known extreme dynamic range of 30 orders of magnitude that causes severe numerical implementation problems for device simulation programs.

$$\sqrt{N_c \cdot N_v} = \exp\left(45.13 + 0.75 \cdot \ln\left(\frac{m_n^*}{m_o} \cdot \frac{m_p^*}{m_o} \cdot \left(\frac{T}{300\ \text{K}}\right)^2\right)\right) \text{cm}^{-3}. \tag{19}$$

With (13) and (19) it is now straightforward to compute the numerical values for the density of states. At room temperature, we have $N_c = 5.1 \cdot 10^{19}$ cm^{-3} and $N_v = 2.9 \cdot 10^{19}$ cm^{-3}; at liquid-nitrogen temperature, we obtain $N_c = 5.8 \cdot 10^{18}$ cm^{-3} and $N_v = 2.5 \cdot 10^{18}$ cm^{-3}.

It should be noted that (7) is only valid for moderate impurity concentrations. For heavy doping the assumption of a localized ionization energy definitely does not hold. Instead an impurity band is formed that may merge with the respective band edge, e.g., [38], [55]. Just modeling a temperature dependence of the ionization energies will not account adequately for the underlying physics in this case. It appears to be appropriate to assume total ionization for concentrations above some threshold value and to account for a suitable functional transition between the classical formulas of (7) and total ionization. All concepts to tackle this problem that have come to my attention so far, however, make use of a very simplistic, not to say alchemical, approach. In MINIMOS 4 these threshold concentrations are 10^{18} cm^{-3} and 10^{19} cm^{-3}, respectively. For a dopant concentration below the lower threshold concentration, the respective of (7) is used to compute the ionized dopant concentration; for a dopant concentration above the higher threshold concentration, complete ionization is assumed. In the interval between the two threshold concentrations, linear interpolation is performed on the fraction of ionization to obtain a smooth transition between partial and complete ionization. Anyway, it should be noted that freeze-out is of major importance only for depletion-mode devices and devices with a partially compensated channel doping [32]. In view of this dilemma with heavy doping one may for many applications well use asymptotic approximations for the Fermi function given by (10) and its inverse given by (16) (see [57]). This is not in contradiction to the partial ionization model given with (6)–(19).

C. Modeling Carrier Mobilities

The next set of physical parameters to be considered carefully for low-temperature simulation consists of the carrier mobilities μ_n and μ_p in (4) and (5). The models for the carrier mobilities have to take into account a great variety of scattering mechanisms the most basic one of which is lattice scattering. The lattice mobility in pure silicon can be fitted with simple power laws.

$$\mu_n^L = 1430 \frac{\text{cm}^2}{\text{Vs}} \cdot \left(\frac{T}{300\ \text{K}}\right)^{-2}$$
$$\mu_p^L = 460 \frac{\text{cm}^2}{\text{Vs}} \cdot \left(\frac{T}{300\ \text{K}}\right)^{-2.18}. \tag{20}$$

The expressions of (20) fit well the experimental data of [2], [15], and [47].

The next effect to be considered is ionized impurity scattering. The best established procedure for this task is to take the functional form of (21) of the fit provided by Caughey and Thomas [16] and use temperature-dependent coefficients.

$$\mu_{n,p}^{LI} = \mu_{n,p}^{\min} + \frac{\mu_{n,p}^{L} - \mu_{n,p}^{\min}}{1 + (CI/C_{n,p}^{\text{ref}})^{\alpha_{n,p}}} \tag{21}$$

$$\mu_n^{\min} = \begin{cases} 80 \dfrac{\text{cm}^2}{\text{Vs}} \cdot \left(\dfrac{T}{300\text{ K}}\right)^{-0.45}, \\ \quad T \geq 200\text{ K} \\ 80 \dfrac{\text{cm}^2}{\text{Vs}} \left(\dfrac{200\text{ K}}{300\text{ K}}\right)^{-0.45} \cdot \left(\dfrac{T}{200\text{ K}}\right)^{-0.15}, \\ \quad T < 200\text{ K} \end{cases} \tag{22}$$

$$\mu_p^{\min} = \begin{cases} 45 \dfrac{\text{cm}^2}{\text{Vs}} \cdot \left(\dfrac{T}{300\text{ K}}\right)^{-0.45}, \\ \quad T \geq 200\text{ K} \\ 45 \dfrac{\text{cm}^2}{\text{Vs}} \left(\dfrac{200\text{ K}}{300\text{ K}}\right)^{-0.45} \cdot \left(\dfrac{T}{200\text{ K}}\right)^{-0.15}, \\ \quad T < 200\text{ K} \end{cases} \tag{23}$$

$$C_n^{\text{ref}} = 1.12 \cdot 10^{17}\text{ cm}^{-3} \cdot \left(\frac{T}{300\text{ K}}\right)^{3.2}$$

$$C_p^{\text{ref}} = 2.23 \cdot 10^{17}\text{ cm}^{-3} \cdot \left(\frac{T}{300\text{ K}}\right)^{3.2} \tag{24}$$

$$\alpha_{n,p} = 0.72 \cdot \left(\frac{T}{300\text{ K}}\right)^{0.065}. \tag{25}$$

The fits for (22)–(25) are from [36]. Similar data have been provided in [6] and [24].

In view of partial ionization one should consider neutral impurity scattering [57]. However, in view of the uncertainty of the quantitative values for ionized impurity scattering, it seems not to be worthwhile to introduce another scattering mechanism with additional fitting parameters. Furthermore, partial ionization appears to be a second-order effect even at liquid-nitrogen temperature. It seems therefore justified to include partial ionization only in the space-charge model and not in the carrier mobilities.

Surface scattering is modeled with an expression suggested by Seavey [54].

$$\mu_{n,p}^{LIS} = \frac{\mu_{n,p}^{\text{ref}} + (\mu_{n,p}^{LI} - \mu_{n,p}^{\text{ref}}) \cdot (1 - F(y))}{1 + F(y) \cdot (S_{n,p}/S_{n,p}^{\text{ref}})^{\alpha_{n,p}}} \tag{26}$$

$$\mu_n^{\text{ref}} = 638 \frac{\text{cm}^2}{\text{Vs}} \cdot \left(\frac{T}{300\text{ K}}\right)^{-1.19}$$

$$\mu_p^{\text{ref}} = 160 \frac{\text{cm}^2}{\text{Vs}} \cdot \left(\frac{T}{300\text{ K}}\right)^{-1.09} \tag{27}$$

with

$$F(y) = \frac{2 \cdot \exp\left(-(y/y^{\text{ref}})^2\right)}{1 + \exp\left(-2 \cdot (y/y^{\text{ref}})^2\right)} \tag{28}$$

$$S_n = \max\left(0, \frac{\partial \psi}{\partial y}\right), \qquad S_p = \max\left(0, -\frac{\partial \psi}{\partial y}\right). \tag{29}$$

S_n^{ref} is assumed to be $7 \cdot 10^5$ V/cm, S_p^{ref} is $2.7 \cdot 10^5$ V/cm, and y^{ref} is 10 nm.

The formulas for surface scattering are definitely not the ultimate expressions. They just fit quite reasonably with experimental observations. Other approaches with the same claim can be found in, e.g., [7], [39], [49]. A U-shaped mobility behavior as found in [8], [10] has not been synthesized because I believe in a different origin than surface scattering for this experimental observation. It should, however, be noted that soft turn-on at liquid-nitrogen temperature has been successfully simulated with a U-shaped mobility expression [27].

Velocity saturation is modeled with (30). These are again fits to experimental data with, however, a theoretical background considering their functional form [2], [42], [43].

$$\mu_n^{LISE} = \frac{2 \cdot \mu_n^{LIS}}{1 + \sqrt{1 + \left(\dfrac{2 \cdot \mu_n^{LIS} \cdot E_n}{v_n^{\text{sat}}}\right)^2}}$$

$$\mu_p^{LISE} = \frac{\mu_p^{LIS}}{1 + \dfrac{\mu_p^{LIS} \cdot E_p}{v_p^{\text{sat}}}} \tag{30}$$

E_n and E_p are the effective driving forces given by (31). Their derivation can be found in [34].

$$E_n = \left|\text{grad}\,\psi - \frac{1}{n} \cdot \text{grad}\,(Ut_n \cdot n)\right|$$

$$E_p = \left|\text{grad}\,\psi + \frac{1}{p} \cdot \text{grad}\,(Ut_p \cdot p)\right|. \tag{31}$$

The saturation velocities are given in the following:

$$v_n^{\text{sat}} = 1.45 \cdot 10^7 \frac{\text{cm}}{\text{s}} \cdot \sqrt{\tanh\left(\frac{155\text{ K}}{T}\right)}$$

$$v_p^{\text{sat}} = 9.05 \cdot 10^6 \frac{\text{cm}}{\text{s}} \cdot \sqrt{\tanh\left(\frac{312\text{ K}}{T}\right)}. \tag{32}$$

The functional form of these fits is after [2]; the experimental data matched are from [2], [14], [15], [22]. An eventual dependence on the crystallographic orientation that one would deduce from [3], [5], [45] is presently not taken into account.

D. Modeling Carrier Temperatures

To describe carrier heating properly, one has to account for local carrier temperatures $T_{n,p}$ in the current relations

(4) and (5). This can be achieved by either solving energy conservation equations self-consistently with the basic transport equations or by using a model obtained by series expansions of the solution to the energy conservation equations [34]. I believe that the latter is sufficient for silicon devices. For the electronic voltages, we have (33) as an approximation. Confirming theoretical investigations can be found in [1].

$$Ut_{n,p} = \frac{k \cdot T_{n,p}}{q} = Ut_o + \frac{2}{3} \cdot \tau^{\epsilon}_{n,p} \cdot \left(v^{\mathrm{sat}}_{n,p}\right)^2 \cdot \left(\frac{1}{\mu^{LISE}_{n,p}} - \frac{1}{\mu^{LIS}_{n,p}}\right). \tag{33}$$

The energy relaxation times $\tau^{\epsilon}_{n,p}$ are in the order of 0.5 ps and just weakly temperature dependent [11]. They should, however, be modeled as functions of the local doping concentration as motivated by the following reasoning. The product of carrier mobility times electronic voltage that symbolizes a diffusion coefficient must be a decreasing function with increasing carrier voltage (see also [11]). Its maximum is attained at thermal equilibrium. Relation (34) must therefore hold.

$$\mu^{LISE}_{n,p} \cdot Ut_{n,p} \leq \mu^{LIS}_{n,p} \cdot Ut_o. \tag{34}$$

Note that models for carrier diffusion coefficients are not required in the basic current relations of (4) and (5).

Substituting (33) into (34) and rearranging terms, one obtains (35) for the energy relaxation times.

$$\tau^{\epsilon}_{n,p} \leq \frac{3}{2} \cdot Ut_o \cdot \frac{\mu^{LIS}_{n,p}}{\left(v^{\mathrm{sat}}_{n,p}\right)^2}. \tag{35}$$

In MINIMOS 4 the energy relaxation times are modeled on the basis of (35) with a fudge factor γ in the range [0, 1] and a default value of 0.8.

$$\tau^{\epsilon}_{n,p} = \gamma \cdot \frac{3}{2} \cdot Ut_o \cdot \frac{\mu^{LIS}_{n,p}}{\left(v^{\mathrm{sat}}_{n,p}\right)^2}. \tag{36}$$

For vanishing doping, one obtains the maximum energy relaxation times, which at 300 K are $\tau^{\epsilon}_n = 4.44 \cdot 10^{-13}$ s, $\tau^{\epsilon}_p = 2.24 \cdot 10^{-13}$ s and at liquid-nitrogen temperature are $\tau^{\epsilon}_n = 8.82 \cdot 10^{-13}$ s, $\tau^{\epsilon}_p = 8.68 \cdot 10^{-13}$ s.

E. Modeling Carrier Generation/Recombination

Thermal generation/recombination at 77 K can be modeled the same way as at 300 K [57]. A comment should be made on the model for the impact ionization rate which has to be supplied for the continuity equations (2) and (3). It still seems, though under heavy dispute in the scientific community, that the old Chynoweth formulation (37) of impact ionization can be used quite satisfactorily for device simulation.

$$R^{II} = -\alpha_n \cdot \frac{|\vec{J}_n|}{q} - \alpha_p \cdot \frac{|\vec{J}_p|}{q} \tag{37}$$

with

$$\alpha_{n,p} = \alpha^{\infty}_{n,p} \cdot \exp\left(-\frac{\beta_{n,p}}{E}\right). \tag{38}$$

The coefficients of (38) can be modeled as temperature dependent by (39) and (40) to fit experimental data [20], [23], [50]. It should be noted that there is some lack of data for liquid-nitrogen temperature, cf. [64]. However, it seems that this impact ionization model is probably somewhat too pessimistic for a proper quantitative prediction of substrate currents as already stated in [46], [59].

$$\alpha^{\infty}_n = 7 \cdot 10^5\ \mathrm{cm}^{-1} \cdot \left(0.57 + 0.43 \cdot \left(\frac{T}{300\ \mathrm{K}}\right)^2\right)$$
$$\alpha^{\infty}_p = 1.58 \cdot 10^6\ \mathrm{cm}^{-1} \cdot \left(0.58 + 0.42 \cdot \left(\frac{T}{300\ \mathrm{K}}\right)^2\right) \tag{39}$$

$$\beta_n = 1.23 \cdot 10^6\ \frac{\mathrm{V}}{\mathrm{cm}} \cdot \left(0.625 + 0.375 \cdot \left(\frac{T}{300\ \mathrm{K}}\right)\right)$$
$$\beta_p = 2.04 \cdot 10^6\ \frac{\mathrm{V}}{\mathrm{cm}} \cdot \left(0.67 + 0.33 \cdot \left(\frac{T}{300\ \mathrm{K}}\right)\right). \tag{40}$$

The Auger coefficients for the model of Auger recombination given in (41) can also be made weakly temperature dependent with (42). The fit has been made to the data of [26].

$$R^{AU} = \left(C_{cn} \cdot n + C_{cp} \cdot p\right) \cdot \left(n \cdot p - n_i^2\right) \tag{41}$$

$$C_{cn} = 2.8 \cdot 10^{-31}\ \frac{\mathrm{cm}^6}{\mathrm{s}} \cdot \left(\frac{T}{300\ \mathrm{K}}\right)^{0.14}$$
$$C_{cp} = 9.9 \cdot 10^{-32}\ \frac{\mathrm{cm}^6}{\mathrm{s}} \cdot \left(\frac{T}{300\ \mathrm{K}}\right)^{0.2}. \tag{42}$$

III. Numerical Aspects

Almost none of the many device simulation programs that have proven their usefulness for room-temperature simulations can be directly applied to low-temperature applications. The primary reason for this is the scaling of carrier concentrations with all thereby-induced consequences. Briefly sketched: De Mari recommended in an early paper [21] to scale the intrinsic carrier concentration to unity, which contributes to change the basic semiconductor equations into a dimensionless form very convenient for computer implementation. Due to the fact that the intrinsic carrier concentration at liquid-nitrogen temperature is in the order of 10^{-20} cm^{-3} (cf. Fig. 3), it is obviously not applicable for scaling in this case, since, for instance, an impurity concentration of 10^{20} cm^{-3} would then be scaled to 10^{40}. To scale the maximum impurity concentration to unity as recommended in the elaborate mathematical book of Markowich [48] is also not feasible, since the scaled intrinsic concentration would be

in the order of 10^{-40}. A way out of this dilemma is to use the concentration C_s defined by (43) for scaling.

$$C_s = \sqrt{4.8 \cdot 10^{22}\ \mathrm{cm}^{-3} \cdot n_i}. \tag{43}$$

The magic concentration in (43) is the number of silicon atoms per cubic centimeter. It serves as an absolute upper limit for the maximum possible concentration of any type. At 300 K temperature, $C_s = 2.58 \cdot 10^{16}\ \mathrm{cm}^{-3}$; at 77 K temperature, $C_s = 3.51 \cdot 10^{1}\ \mathrm{cm}^{-3}$. This scaling equilibrates the relevant concentrations and thus is optimal for avoiding fatal floating point underflow or overflow exceptions.

A further detail to be considered for numerical implementation is the appropriate approximation of the inverse Fermi function $G_{1/2}(x)$. A convenient fit is given by (44).

$$G_{1/2}(x) = \frac{\ln(x)}{1 - x^2} + \frac{\left(\frac{3 \cdot \sqrt{\pi} \cdot x}{4}\right)^{2/3}}{1 + \frac{1}{\left(0.24 + 1.08 \cdot \left(3 \cdot \sqrt{\pi} \cdot x/4\right)^{2/3}\right)^2}}. \tag{44}$$

The first term in (44) has to be replaced by a truncated series expansion if the argument x is in the vicinity of 1.

$$\frac{\ln(x)}{1 - x^2} = \frac{x - 2}{2} + O\left((x - 1)^2\right). \tag{45}$$

A review about approximations to Fermi functions and their inverse functions can be found in [12], [18], [57].

IV. A Glimpse of Results

Results of investigations about submicrometer n-channel enhancement-mode MOSFET's at room and liquid-nitrogen ambient temperatures are presented. A single drain technology designed for well functioning devices at room-temperature operation with 3/4-μm gate length (0.39-μm metallurgical channel length) has been analyzed where the gate length has been reduced for liquid-nitrogen temperature operation to 0.51 μm (0.15-μm metallurgical channel length). The gate oxide thickness is 9 nm, and the work function of the donor doped gate polysilicon is −570 mV. A window of the critical drain profile corner is depicted in Fig. 4.

The actual analysis has been carried out with MINIMOS 4, which is a further development of the MINIMOS program [34], [53], [56] to include quantitative capabilities for low-temperature simulation.

The threshold voltage versus gate length L is shown in Fig. 5 for this particular technology. The long-channel threshold voltage is about 580 mV at 77 K and about 340 mV at room temperature. Threshold voltage is here defined as the gate voltage required to achieve a drain current of 0.1 μA · W/L at a given drain bias. No substrate bias has been applied for these investigations. It appears to be a matter of taste whether to use the gate length L or the metallurgical channel length for this kind of investigation. However, device designers usually prefer the gate length.

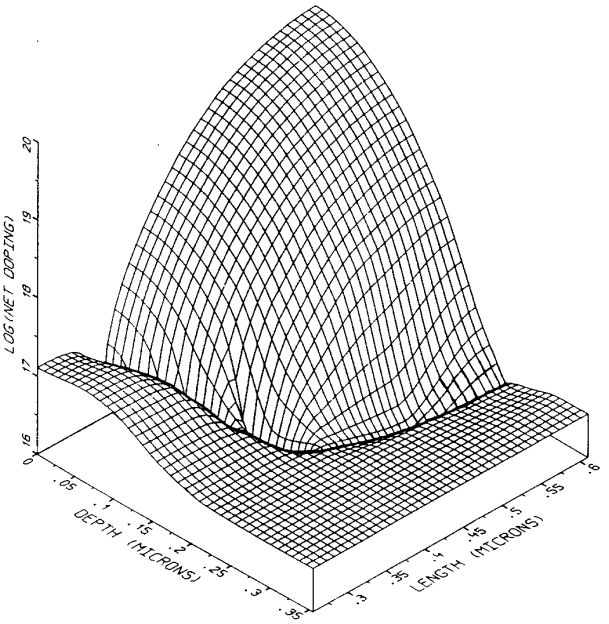

Fig. 4. Detail of net impurity profile.

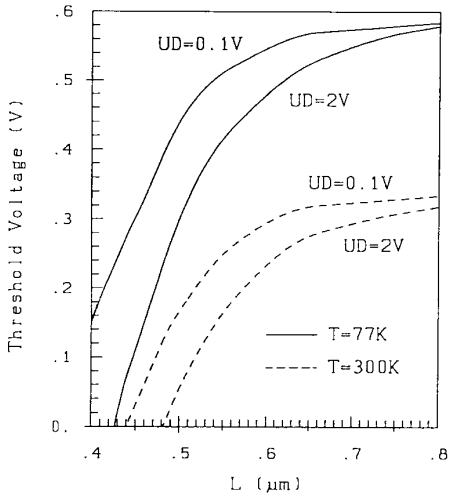

Fig. 5. Threshold voltage versus gate length.

Fig. 6 shows the simulated subthreshold characteristics for two different drain biases (UD = 0.1 V, UD = 2 V, UB = 0 V) at room and liquid-nitrogen temperatures. The subthreshold slope is obviously much steeper at liquid-nitrogen temperature with about 25 mV/decade compared to 95 mV/decade at room temperature. It is interesting that the improvement of the slope is almost as good as 3.9 the ratio of 300 K/77 K [41]. Furthermore, the shift of the subthreshold characteristics between low and

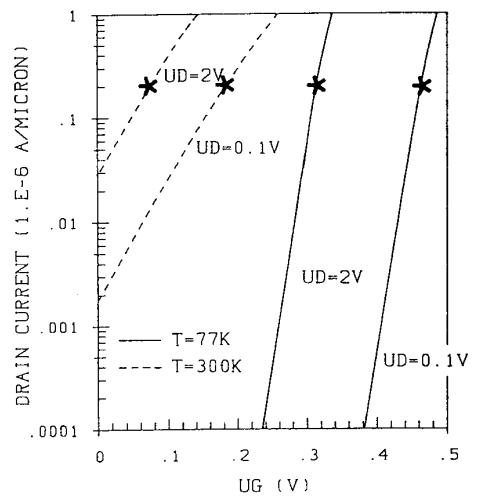

Fig. 6. Simulated subthreshold characteristics. The asterisks indicate the respective threshold voltages.

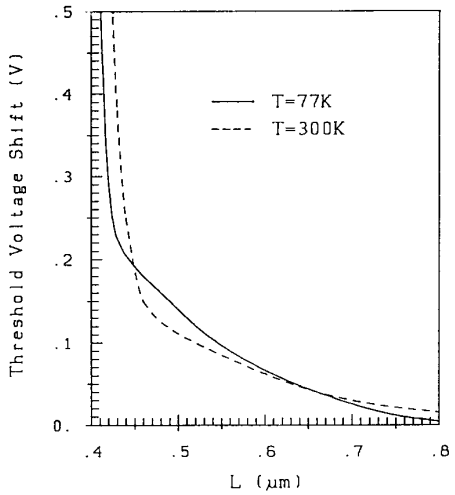

Fig. 7. Drain-bias-induced threshold voltage shift versus gate length.

high drain bias, which should be primarily due to drain-induced surface barrier lowering, is about 50 mV larger at 77 K compared to the room-temperature shift. To have a larger influence of drain-induced barrier lowering at lower temperature is in contradiction with the sound results of [67]. The observed phenomenon therefore must be of different origin. In order to get insight into this effect, the drain-bias-induced threshold voltage shift has been computed as a function of gate length. Fig. 7 shows this shift of the threshold voltage between $UD = 0.1$ V and $UD = 2$ V for this technology. One can nicely see that the functional behavior is caused by two overlapping phenomena with a knee at a gate length of 0.43 μm at 77 K and 0.46 μm at 300 K. Detailed investigations have brought up several interacting causes. One is partial freeze-out of acceptors in the bulk below the channel, which leads to an increase of built-in potential and thus to increasing depletion widths with decreasing temperature [44], [66]. This reasoning is partially confirmed in [30]. The second cause is the formation of a sort of parasitic channel by impact ionization, which has also been reported in [53].

Figs. 8 and 9 show the simulated output characteristics for four different gate biases. If we take current output for the same gate drive as a measure of device quality, the low-temperature operation resulted in approximately a 50 percent improvement compared to room-temperature operation. Similar results have been experimentally obtained (cf. [62]). This improvement decreases with shrinking channel length as observed in [52].

In the following a few results about the distribution of the various physical quantities in the interior of the device will be presented. The off-state at $UG = 0$ V, $UD = 2$ V is depicted with the electron concentration given by Figs. 10 and 11 at liquid-nitrogen temperature and room temperature, respectively. It is easily visible that the device is not satisfactorily off at room temperature. The channel is perfectly depleted at 77 K.

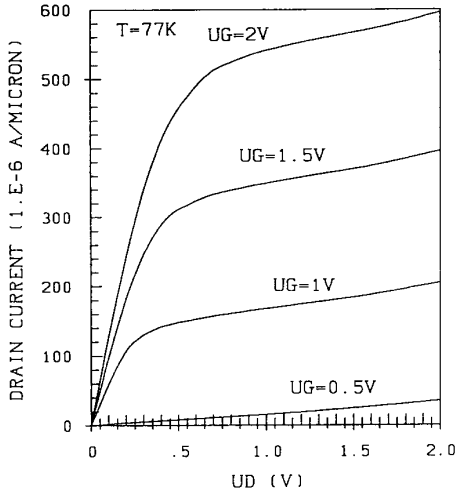

Fig. 8. Simulated output characteristics at 77 K.

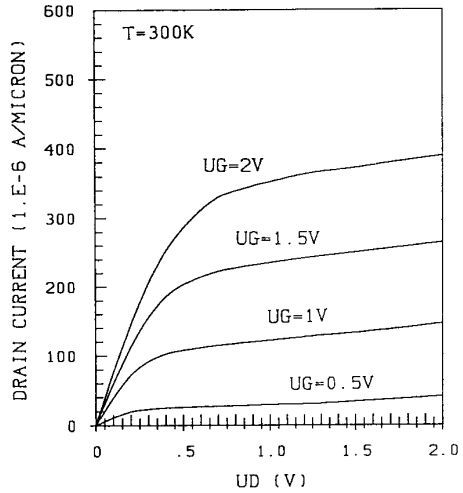

Fig. 9. Simulated output characteristics at 300 K.

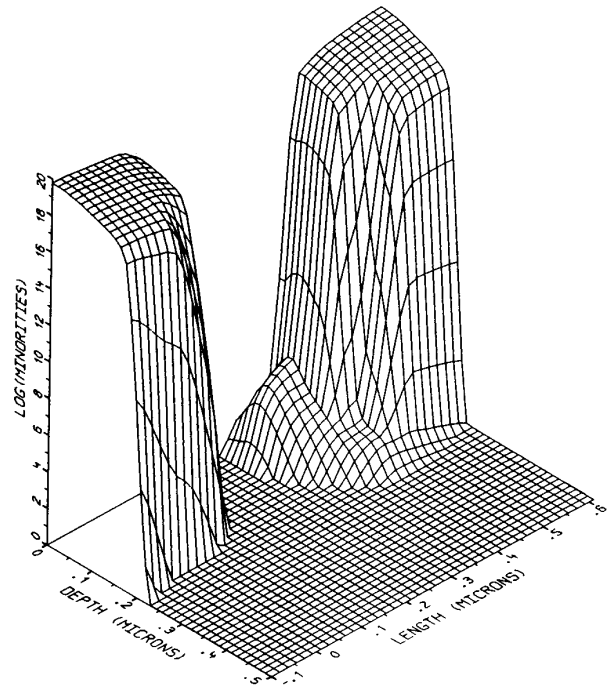

Fig. 10. Electron concentration at 77 K (UG = 0 V, UD = 2 V).

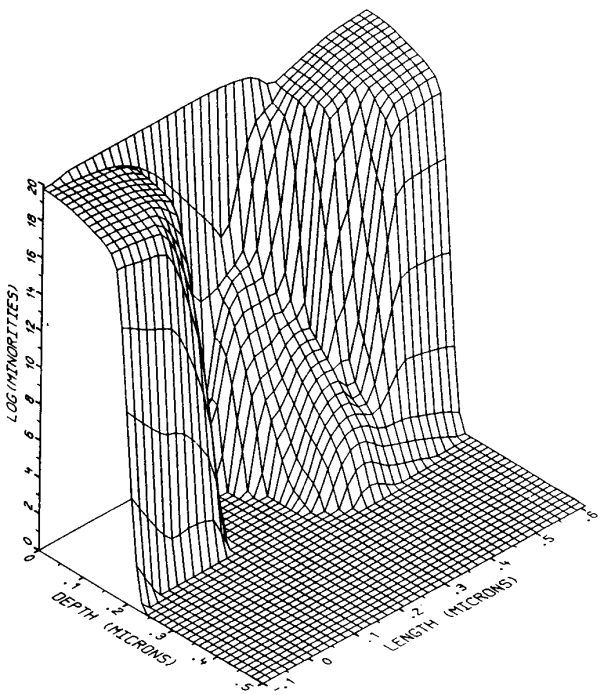

Fig. 12. Electron concentration at 77 K (UG = 2 V, UD = 2 V).

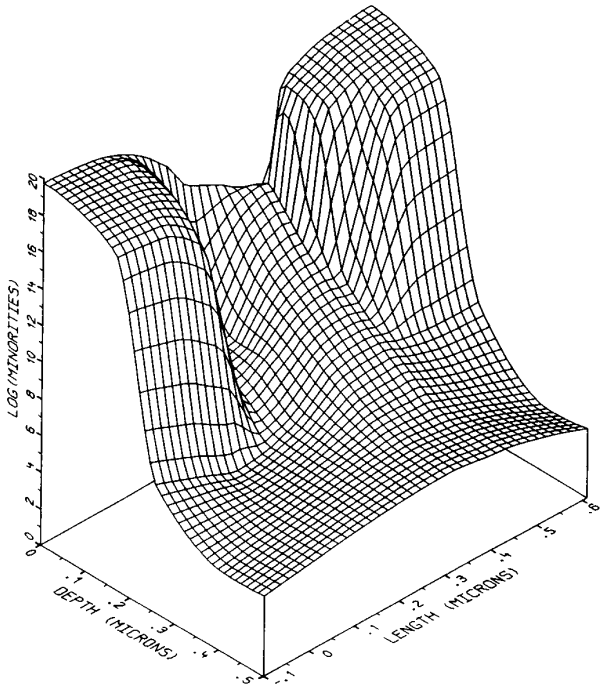

Fig. 11. Electron concentration at 300 K (UG = 0 V, UD = 2 V).

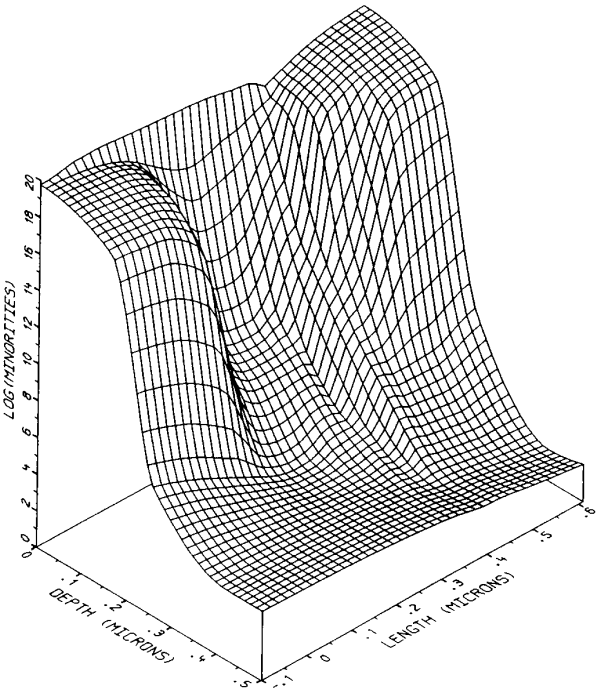

Fig. 13. Electron concentration at 300 K (UG = 2 V, UD = 2 V).

The one-state is documented with a bias of UG = 2 V, UD = 2 V. Figs. 12 and 13 show again the electron concentration at liquid-nitrogen temperature and room temperature, respectively. One can nicely observe the inverse layer that is much steeper for the low-temperature simulation. Furthermore, one can see that there are considerably more electrons generated by impact ionization close to the drain.

The impact ionization rates are shown in Figs. 14 and 15. The peak concentration that occurs in both cases at

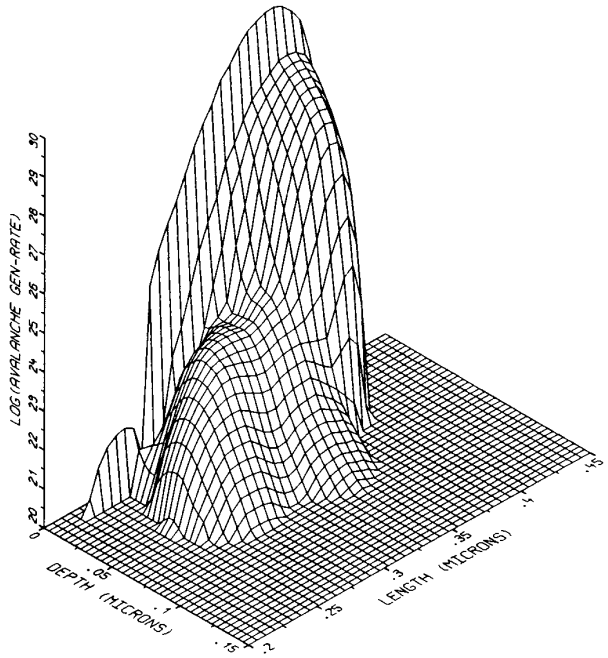

Fig. 14. Impact ionization rate at 77 K (UG = 2 V, UD = 2 V).

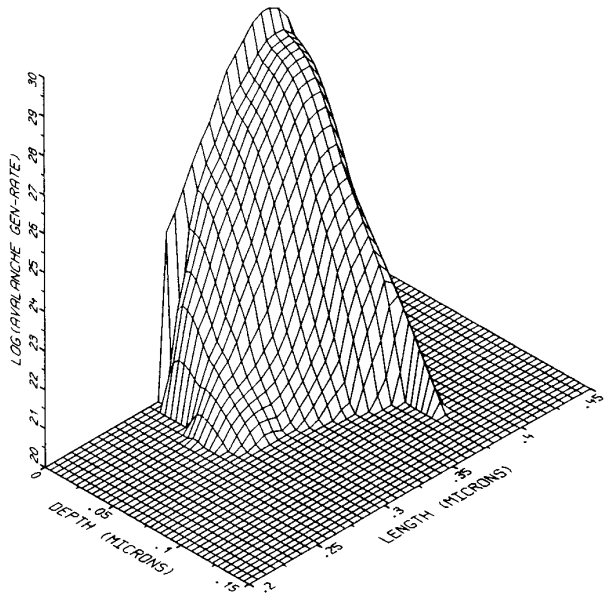

Fig. 15. Impact ionization rate at 300 K (UG = 2 V, UD = 2 V).

the surface is almost two orders of magnitude higher for low-temperature operation. The substrate current to drain current ratio is increased by a factor of 5.2, which is fairly high for n-channel devices [4].

Figs. 16 and 17 show the distribution of electron temperature at 77 and 300 K ambient temperature, respectively. The maximum temperature is 213 K at 77 K and 2220 K at room temperature. This maximum is in both

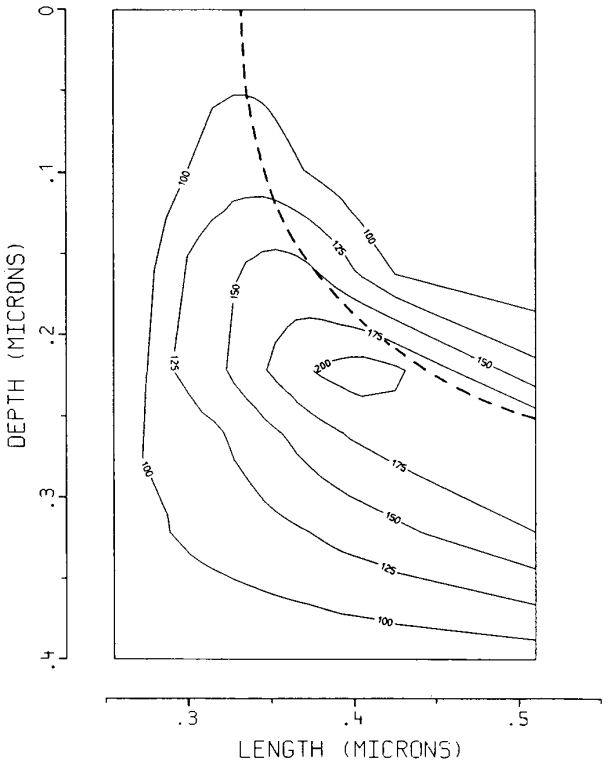

Fig. 16. Electron temperature at 77 K (UG = 2 V, UD = 2 V).

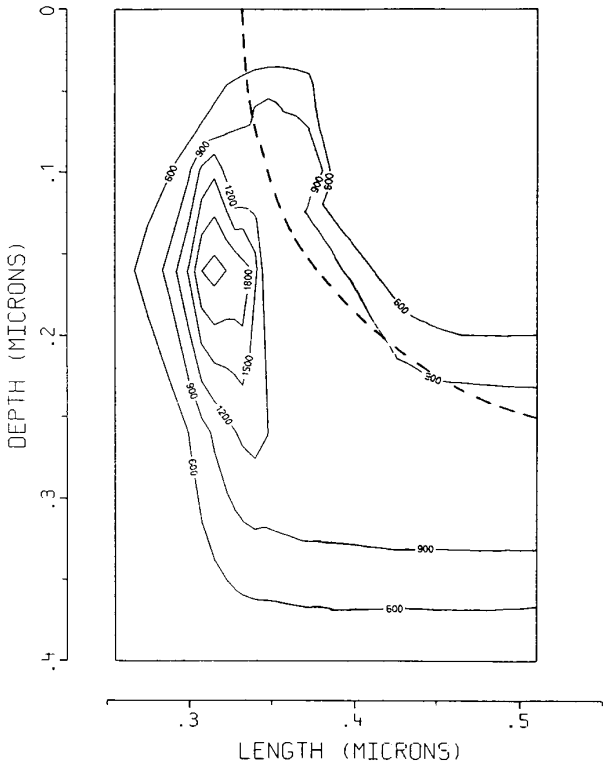

Fig. 17. Electron temperature at 300 K (UG = 2 V, UD = 2 V).

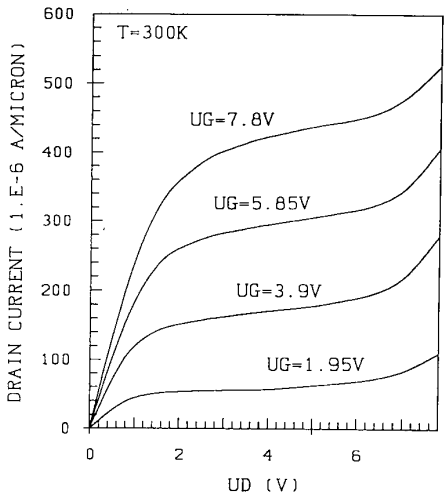

Fig. 18. Simulated output characteristics at 300 K for up-scaled device.

cases located in the reverse-biased drain substrate diode with a smooth transition into the channel. The position of the maximum is deeper in the substrate and closer to the drain area at 77 K compared to the room-temperature result. It is worthwhile to note that the channel charge stays nearly thermal close to the interface. The phenomenon of smaller carrier heating at liquid-nitrogen temperature is a result of a smoother distribution and a smaller maximum of the driving force. Smaller carrier heating at 77 K has been confirmed by many simulations. However, remembering various private communications, it is not really expected, particularly in view of larger energy relaxation times at liquid-nitrogen temperature.

One numerical experiment carried out concerns scaling. The device under investigation has been scaled up by a factor of $3.9 = 300\ \mathrm{K}/77\ \mathrm{K}$ using the classical MOS device scaling rules. Fig. 18 shows the simulated output characteristics for the up-scaled device. We can see that such temperature scaling is relatively crude. The current drive capability is not achieved, since the threshold voltage does not scale [61]. Furthermore, avalanche breakdown is more dominant as indicated by the bending of the characteristics. The output conductance in the saturation region, however, scales very well.

Similar investigations for a lightly doped drain technology can be found in [59].

The question remains of how good these simulation results agree with measurements. The device presented has not been fabricated with 0.51-μm gate length. Satisfactory agreement has been achieved for devices down to 3/4-μm gate length. To be able to judge rigorously the agreement between measurement and simulation at low temperatures, one should also look at results obtained with different programs. These can be found, e.g., in [35] for a modified version of CADDET, in [52], [63] for a modified version of FIELDAY, and in [67] for a modified version of GEMINI.

Acknowledgment

I am indebted to Prof. H. Pötzl for many critical and stimulating discussions.

References

[1] N. Ahmad and V. K. Arora, "Velocity-field profile on n-silicon: A theoretical analysis," *IEEE Trans. Electron Devices*, vol. ED-33, pp. 1075-1077, 1986.

[2] M. Ali-Omar and L. Reggiani, "Drift and diffusion of charge carriers in silicon and their empirical relation to the electric field," *Solid-State Electron.*, vol. 30, pp. 693-697, 1987.

[3] M. Aoki, K. Yano, T. Masuhara, S. Ikeda, and S. Meguro, "Optimum crystallographic orientation of submicron CMOS devices," in *IEDM Tech. Dig.*, 1985, pp. 557-580.

[4] M. Aoki, S. Hanamura, T. Masuhara, and K. Yano, "Performance and hot-carrier effects of small CRYO-CMOS devices," *IEEE Trans. Electron Devices*, vol. ED-34, pp. 8-18, 1987.

[5] M. Aoki, K. Yano, T. Masuhara, S. Ikeda, and S. Meguro, "Optimum crystallographic orientation of submicrometer CMOS devices operated at low temperatures," *IEEE Trans. Electron Devices*, vol. ED-34, pp. 52-57, 1987.

[6] N. D. Arora, J. R. Hauser, and D. J. Roulston, "Electron and hole mobilities in silicon as a function of concentration and temperature," *IEEE Trans. Electron Devices*, vol. ED-29, pp. 292-295, 1982.

[7] N. D. Arora and G. S. Gildenblat, "A semi-empirical model of the MOSFET inversion layer mobility for low-temperature operation," *IEEE Trans. Electron Devices*, vol. ED-34, pp. 89-93, 1987.

[8] G. Baccarani and M. R. Wordeman, "Transconductance degradation in thin-oxide MOSFET's," in *IEDM Tech. Dig.*, 1982, pp. 278-281.

[9] G. Baccarani, "Physics of submicron devices," in *Proc. VLSI Process and Device Modeling* (Katholieke Universiteit Leuven, Belgium), 1983, pp. 1-23.

[10] G. Baccarani and M. R. Wordeman, "Transconductance degradation in thin-oxide MOSFET's," *IEEE Trans. Electron Devices*, vol. ED-30, pp. 1295-1304, 1983.

[11] ——, "An investigation of steady-state velocity overshoot in silicon," *Solid-State Electron.*, vol. 28, pp. 407-416, 1985.

[12] J. S. Blakemore, "Approximations for Fermi-Dirac integrals, especially the function $F1/2(x)$ used to describe electron density in a semiconductor," *Solid-State Electron.*, vol. 25, pp. 1067-1076, 1982.

[13] K. Blotekjaer, "Transport equations for electrons in two-valley semiconductors," *IEEE Trans. Electron Devices*, vol. ED-17, pp. 38-47, 1970.

[14] C. Canali and G. Ottaviani, "Saturation values of the electron drift velocity in silicon between 300 K and 4.2 K," *Phys. Lett.*, vol. 32A, pp. 147-148, 1970.

[15] C. Canali, G. Majni, R. Minder, and G. Ottaviani, "Electron and hole drift velocity measurements in silicon and their empirical relation to electric field and temperature," *IEEE Trans. Electron Devices*, vol. ED-22, pp. 1045-1047, 1975.

[16] D. M. Caughey and R. E. Thomas, "Carrier mobilities in silicon empirically related to doping and field," *Proc. IEEE*, vol. 52, pp. 2192-2193, 1967.

[17] M. Chrzanowska-Jeske and R. C. Jaeger, "Modeling of temperature dependent transport parameters for low temperature bipolar transistor simulation," in *Proc. Symp. Low Temperature Electronics and High Temperature Superconductors* (Electrochem. Soc.), vol. 88-9, 1988, pp. 30-38.

[18] W. J. Cody and H. C. Thacher, "Rational Chebyshev approximations for Fermi-Dirac integrals of orders $-1/2$, $1/2$, and $3/2$," *Math. Comp.*, vol. 21, pp. 30-40, 1967.

[19] L. M. Colonna-Romano and R. D. Deverell, "Operation of a CMOS microprocessor while immersed in liquid nitrogen," *IEEE J. Solid-State Circuits*, vol. SC-21, pp. 491-492, 1986.

[20] C. R. Crowell and S. M. Sze, "Temperature dependence of avalanche multiplication in semiconductors," *Appl. Phys. Lett.*, vol. 9, pp. 242-244, 1966.

[21] A. DeMari, "An accurate numerical steady-state one-dimensional solution of the P-N junction," *Solid-State Electron.*, vol. 11, pp. 33-58, 1968.

[22] P. P. Debye and E. M. Conwell, "Electrical properties of N-type germanium," *Phys. Rev.*, vol. 93, pp. 693-706, 1954.

[23] D. R. Decker and C. N. Dunn, "Temperature dependence of carrier

ionization rates and saturated velocities in silicon," *J. Electron. Mater.*, vol. 4, pp. 527-547, 1975.
[24] J. M. Dorkel and P. Leturcq, "Carrier mobilities in silicon semi-empirically related to temperature, doping and injection level," *Solid-State Electron.*, vol. 24, pp. 821-825, 1981.
[25] D. W. Duke, "Use of the ETA-10 supercomputer: A status report," in *Proc. Symp. Low Temperature Electronics and High Temperature Superconductors* (Electrochem. Soc.), vol. 88-9, 1988, pp. 30-38.
[26] J. Dziewior and W. Schmid, "Auger coefficients for highly doped and highly excited silicon," *Appl. Phys. Lett.*, vol. 31, pp. 346-348, 1977.
[27] J. Faricelli, private communication, 1987.
[28] J. Frey, "Transport physics for VLSI," in *Introduction to the Numerical Analysis of Semiconductor Devices and Integrated Circuits*. Dublin, Boole Press, 1981, pp. 51-57.
[29] F. H. Gaensslen, R. C. Jaeger, and J. J. Walker, "Low-temperature threshold behavior of depletion mode devices," in *IEDM Tech. Dig.*, 1976, pp. 520-524.
[30] F. H. Gaensslen, V. L. Rideout, E. J. Walker, and J. J. Walker, "Very small MOSFET's for low temperature operation," *IEEE Trans. Electron Devices*, vol. ED-24, pp. 218-229, 1977.
[31] F. H. Gaensslen and R. C. Jaeger, "Temperature dependent threshold behaviour of depletion mode MOSFET's," *Solid-State Electron.*, vol. 22, pp. 423-430, 1979.
[32] ——, "Behavior of electrically small depletion mode MOSFET's at low temperature," *Solid-State Electron.*, vol. 24, pp. 215-220, 1981.
[33] H. K. Gummel, "A self-consistent iterative scheme for one-dimensional steady state transistor calculations," *IEEE Trans. Electron Devices*, vol. ED-11, pp. 455-465, 1964.
[34] W. Hänsch and S. Selberherr, "MINIMOS 3: A MOSFET simulator that includes energy balance," *IEEE Trans. Electron Devices*, vol. ED-34, pp. 1074-1078, 1987.
[35] A. K. Henning, N. Chan, and J. D. Plummer, "Substrate current in n-channel and p-channel MOSFET's between 77 K and 300 K: Characterization and simulation," in *IEDM Tech. Dig.*, 1985, pp. 573-576.
[36] A. K. Henning, N. N. Chan, J. T. Watt, and J. D. Plummer, "Substrate current at cryogenic temperatures: Measurements and a two-dimensional model for CMOS technology," *IEEE Trans. Electron Devices*, vol. ED-34, pp. 64-74, 1987.
[37] K. Hess and G. J. Iafrate, "Theory and applications of near ballistic transport in semiconductors," *Proc. IEEE*, vol. 76, pp. 519-532, 1988.
[38] W. Heywang and H. Pötzl, *Bandstruktur und Stromtransport*. Berlin: Springer, 1976.
[39] A. Hiroki, S. Odanaka, K. Ohe, and H. Esaki, "A mobility model for submicrometer MOSFET device simulations," *IEEE Electron Device Lett.*, vol. EDL-8, pp. 231-233, 1987.
[40] R. C. Jaeger, private communication, Oct. 1987.
[41] R. C. Jaeger and F. H. Gaensslen, "Low temperature MOS microelectronics," in *Proc. Symp. Low Temperature Electronics and High Temperature Superconductors* (Electrochem. Soc.), vol. 88-9, 1988, pp. 43-54.
[42] R. Jaggi and H. Weibel, "High-field electron drift velocities and current densities in silicon," *Helv. Phys. Acta*, vol. 42, pp. 631-632, 1969.
[43] R. Jaggi, "High-field drift velocities in silicon and germanium," *Helv. Phys. Acta*, vol. 42, pp. 941-943, 1969.
[44] A. Kamgar, "Miniaturization of Si MOSFET's at 77 K," *IEEE Trans. Electron Devices*, vol. ED-29, pp. 1226-1228, 1982.
[45] M. Kinugawa, M. Kakumu, T. Usami, and J. Matsunaga, "Effects of silicon surface orientation on submicron CMOS devices," in *IEDM Tech. Dig.*, 1985, pp. 581-584.
[46] D. Lau, G. Gildenblat, G. G. Sodini, and D. E. Nelson, "Low-temperature substrate current characterization of n-channel MOSFET's," in *IEDM Tech. Dig.*, 1985, pp. 565-568.
[47] S. S. Li and W. R. Thurber, "The dopant density and temperature dependence of electron mobility and resistivity in n-type silicon," *Solid-State Electron.*, vol. 20, pp. 609-616, 1977.
[48] P. A. Markowich, *The Stationary Semiconductor Device Equations*. New York: Springer, 1986.
[49] T. Nishida and C. T. Sah, "A physically based mobility model for MOSFET numerical simulation," *IEEE Trans. Electron Devices*, vol. ED-34, pp. 310-320, 1987.
[50] Y. Okuto and C. R. Crowell, "Threshold energy effect on avalanche breakdown voltage in semiconductor junctions," *Solid-State Electron.*, vol. 18, pp. 161-168, 1975.
[51] P. J. Robertson and D. J. Dumin, "Ballistic transport and properties of submicrometer silicon MOSFET's from 300 to 4.2 K," *IEEE Trans. Electron Devices*, vol. ED-33, pp. 494-498, 1986.
[52] G. A. Sai-Halasz, "Processing and characterization of ultra small silicon devices," in *Proc. ESSDERC Conf.*, 1987, pp. 71-80.
[53] A. Schütz, S. Selberherr, and H. Pötzl, "Analysis of breakdown phenomena in MOSFET's," *IEEE Trans. Computer-Aided Design of ICAS*, vol. CAD-1, pp. 77-85, 1982.
[54] M. Seavey, private communication, 1987.
[55] K. Seeger, *Semiconductor Physics*. Vienna: Springer, 1973.
[56] S. Selberherr, A. Schütz, and H. Pötzl, "MINIMOS—A two-dimensional MOS transistor analyzer," *IEEE Trans. Electron Devices*, vol. ED-27, pp. 1540-1550, 1980.
[57] S. Selberherr, *Analysis and Simulation of Semiconductor Devices*. New York: Springer, 1984.
[58] S. Selberherr, W. Griebel, and H. Pötzl, "Transport physics for modeling semiconductor devices," in *Simulation of Semiconductor Devices and Processes*. Swansea, U.K.: Pineridge Press, 1984.
[59] S. Selberherr, "Low temperature Mos device modeling," in *Proc. Symp. Low Temperature Electronics and High Temperature Superconductors* (Electrochem. Soc.), vol. 88-9, 1988, pp. 43-86.
[60] G. G. Shahidi, D. A. Antoniadis, and H. I. Smith, "Electron velocity overshoot at 300 K and 77 K in silicon MOSFET's with submicron channel length," in *IEDM Tech. Dig.*, 1986, pp. 824-825.
[61] P. M. Solomon, "Options for high speed logic at 77 K," in *Proc. Symp. Low Temperature Electronics and High Temperature Superconductors* (Electrochem. Soc.), vol. 88-9, 1988, pp. 3-17.
[62] T. Sugano, "Low temperature electronics Research in Japan," in *Proc. Symp. Low Temperature Electronics and High Temperature Superconductors* (Electrochem. Soc.), vol. 88-9, 1988, pp. 18-29.
[63] Y.-C. J. Sun, Y. Taur, R. H. Dennard, and S. P. Klepner, "Submicrometer-channel CMOS for low-temperature operation," *IEEE Trans. Electron Devices*, vol. ED-34, pp. 19-27, 1987.
[64] A. D. Sutherland, "An improved empirical fit to Baraff's universal curves for the ionization coefficients of electron and hole multiplication in semiconductors," *IEEE Trans. Electron Devices*, vol. ED-27, pp. 1299-1300, 1980.
[65] S. M. Sze, *Physics of Semiconductor Devices*. New York: Wiley, 1969.
[66] J. T. Watt, B. J. Fishbein, and J. D. Plummer, "A low-temperature NMOS technology with cesium-implanted load devices," *IEEE Trans. Electron Devices*, vol. ED-34, pp. 28-38, 1987.
[67] J. C. S. Woo and J. D. Plummer, "Short channel effects in MOSFET's at liquid-nitrogen temperature," *IEEE Trans. Electron Devices*, vol. ED-33, pp. 1012-1019, 1986.

*

Siegfried Selberherr (M'79-SM'84) was born in Klosterneuburg, Austria, on August 3, 1955. He received the Diplomingenieur degree in control theory and industrial electronics from the Technical University of Vienna in 1978. He finished his thesis on "Two-Dimensional MOS Transistor Modeling" in 1981 at the Institute für Allgemeine Elektrotechnik und Elektronik (previously the Institut für Physikalische Elektronik) of the Technical University of Vienna.

Since 1978, he has been a Professor at the Technical University of Vienna, and since 1984, has held the *venia docendi* in computer-aided design. Since 1988, he has been the head of the Institut für Mikroelektronik. His current interests are the modeling and simulation of problems for microelectronics engineering. He has authored or coauthored more than 100 papers in journals and conference proceedings and is the author of the book *Analysis and Simulation of Semiconductor Devices*.

Dr. Selberherr is a member of the Association for Computing Machinery, the Society of Industrial and Applied Mathematics, and the Verband deutscher Elektrotechniker. He serves as Editor of the *Transactions of the Society for Computer Simulation*, of *Electrosoft*, of *Mikroelektronik*, and of the Springer-Verlag book series, *Computational Microelectronics*. In 1983, he received the Dr. Ernst Fehrer Award. In 1985, he received the award of the Nachrichtentechnische Gesellschaft, and in 1986, he was honored with the Dr. Herta Firnberg Staatspreis. In 1987, he received the Heinz Zemanek Award.